

# Alternating Dual-Pulse, Dual-Frequency Techniques for Range and Velocity Ambiguity Mitigation on Weather Radars

Sebastián Torres<sup>1</sup>, Richard Passarelli, Jr.<sup>2</sup>, Alan Siggia<sup>2</sup>, and Pentti Karhunen<sup>3</sup>

(1) SMT Consulting, Norman, Oklahoma, USA,

(2) Vaisala Inc., Westford, Massachusetts, USA, (3) Vaisala Oyj, Helsinki, Finland

## 1. Introduction

An intrinsic limitation of pulsed Doppler radars is given by the fact that range coverage and maximum unambiguous Doppler velocity are inversely coupled. That is, trying to improve one necessarily results in worsening the other, and trade-offs are often needed that hamper the observation of severe weather phenomena. Fortunately, significant strides have been made in the development of signal processing methods that mitigate range and velocity ambiguities. For example, two complementary techniques – staggered pulse repetition time (PRT) and SZ-2 systematic phase coding – have been suggested and are currently operational or scheduled for future upgrades of the US NEXRAD network of weather radars (Torres 2005, 2006). Although the performance of these techniques has proven to be quite satisfactory on S-band radars, the problem of range and velocity ambiguities on X- and C-band radars is more severe and more aggressive mitigation approaches must be implemented.

Exploiting the concept of frequency diversity, we propose a family of sampling and signal processing techniques to increase the maximum unambiguous range and velocity product beyond what is achievable with classical methods. Although the use of frequency diversity on weather radars is not new, its application for the mitigation of range and velocity ambiguities has been rather limited.

## 2. Dual-Frequency Doppler Radar

Doviak et al. (1976) first applied the idea of frequency diversity to mitigate range and velocity ambiguities in what they termed *dual-wavelength Doppler radar* whereby coherent signals of slightly different frequencies are transmitted simultaneously and mixed at the receiver. They showed that the resulting “differential” Doppler shift corresponding to the beat frequency  $f_1 - f_2$  is lower than the Doppler shift of either frequency channel, effectively increasing the range of unambiguous velocities. However, the authors questioned the practicality of this approach due to the technological limitations of over three decades ago and the fact that simpler techniques such as staggered PRT exhibit similar performance in reducing ambiguities.

Later, Doviak et al. (1979) extended the dual-wavelength Doppler radar concept proposing closely spaced frequencies that are apart enough to ensure uncorrelated channels. They allowed each frequency channel to transmit a different PRT: a long PRT yielding a large unambiguous range for

reflectivity was proposed for one channel, whereas a short PRT was proposed for velocity estimation on the other channel. This technique is analogous to the (single wavelength) batch mode processing that is currently implemented on the NEXRAD network but has the additional advantage of reducing the acquisition time. Glover et al. (1981) reported an implementation of this dual-frequency technique on a proof-of-concept Doppler weather radar for NEXRAD in which essentially two radars shared one antenna.

Doviak et al. (1979) also suggested replacing the short PRT with staggered PRT sampling to obtain “automatic” velocity dealiasing. However, the practicality and performance of this idea was not explored any further.

## 3. Alternating Dual-Pulse, Dual-Frequency Techniques

Here, we introduce a family of alternating dual-pulse, dual-frequency techniques (ADPDF). These are based on frequency diversity and extend the idea of Doviak et al. (1979) to mitigate range and velocity ambiguities on Doppler weather radars.

### 3.1. ADPDF Sampling

Sampling for the low- and high-frequency channels (denoted by subscripts 1 and 2, respectively) is given in Fig. 1. Here,  $T_1$  and  $T_2$  are the “base” PRTs,  $\delta_1$  and  $\delta_2$  (which are much smaller than  $T_1$  and  $T_2$ ) control PRT staggering on each channel, and  $\delta_0$  is the initial time shift between the two frequency channels.

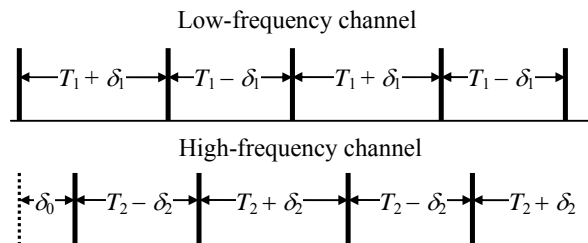


Fig 1. General ADPDF sampling scheme.

A family of ADPDF techniques can be obtained by selecting sampling parameters in different ways. For example, PRT staggering can be eliminated from channels 1 and 2 (i.e., producing uniform PRT) by setting  $\delta_1$  or  $\delta_2$  to 0, respectively. On the other hand, one of the “base” PRTs can be made long enough to eliminate range ambiguities while the other one can be kept short enough to minimize velocity

aliasing as in Doviak et al. (1979). Additionally, it is possible to use the same transmitter for both channels by choosing  $T_1$  and  $T_2$  carefully (e.g.,  $T_1 = T_2$ ) and by increasing  $\delta_0$  so that duty cycle requirements are easily met as a result of the harmonized interlacing of transmitter pulses. This is a clear advantage over the two-transmitter design implemented by Glover et al. (1981).

Regardless of the choice of sampling parameters to minimize the occurrence of range and velocity ambiguities, an additional benefit of frequency diversity is the reduction in acquisition time by a factor of two. This holds if the two frequencies are spaced by more than the reciprocal of the transmitted pulse width so that the two frequency channels are uncorrelated (Doviak and Zrnić 1993). Obviously, these benefits come at a price: (1) the increased complexity to control transmitter pulsing, (2) the additional hardware to receive signals from two frequency channels, and (3) the increased throughput required to process more samples for a given dwell time.

In the next sections, we focus our study to three examples of ADPDF sampling. The first one, herein referred to as ADPDF1, exhibits PRT staggering on both frequency channels, both with the same “base” PRT; sampling parameters are such that  $T_1 = T_2 = T$  and  $\delta_0 = \delta_1 = \delta_2 = \delta$ . The second one, herein referred to as ADPDF2, exhibits uniform PRT on one channel and staggered PRT on the other; sampling parameters are such that  $T_1 = T_2 = T$ ,  $\delta_0 = \delta$ ,  $\delta_1 = 0$ , and  $\delta_2 = 2\delta$ . The last one, herein referred to as ADPDF3, is the same as ADPDF2 except that  $\delta_0 = T/2$ .

### 3.2. ADPDF Doppler Velocity Estimation

Denote the complex signals from the two frequency channels by  $V_1$  and  $V_2$ . The numbers of samples in the dwell time for each channel ( $M_1$  and  $M_2$ ) depend on the sampling parameters. In general,  $M_1$  and  $M_2$  are not the same; however, for the three variations under analysis we can consider  $M_1 = M_2 = M$ .

Doppler velocity is typically estimated from the weather signal autocorrelation at any non-zero lag. In the case of ADPDF signals, we could exploit the particular sampling and use multiple readily-available lags; instead, let's consider the following quantity:

$$R_{\delta_1+\delta_2} = \sum_{m=0}^{M-2} R_{12}(m)R_{12}(m+1), \quad (1)$$

where

$$R_{12}(m) = \begin{cases} V_1^*(m)V_2(m), & m \text{ even} \\ V_1(m)V_2^*(m), & m \text{ odd} \end{cases}; \quad m = 0, \dots, M-1. \quad (2)$$

Note that  $R_{\delta_1+\delta_2}$  is not the autocorrelation function at lag  $\delta_1 + \delta_2$ . However, as shown next, it allows unambiguous Doppler velocity measurements in the same interval as if  $R(\delta_1 + \delta_2)$  were available. After taking the expected value of (1), splitting the sum into its even and odd terms, and using the fact that the signals from the two frequency channels are uncorrelated, we obtain

$$E[R_{\delta_1+\delta_2}] \propto R_1(T_1 + \delta_1)R_2^*(T_2 - \delta_2) + R_1^*(T_1 - \delta_1)R_2(T_2 + \delta_2). \quad (3)$$

Assuming that the weather signal spectrum is Gaussian, that the propagation properties of the signal and the scattering

properties of the atmospheric targets are very similar (i.e., frequencies are closely spaced), and using the fact that for the three techniques under analysis  $\delta_1 + \delta_2 = 2\delta$ , the argument of (3) becomes:

$$\arg\{E[R_{2\delta}]\} \approx -8\pi\bar{v}\delta/\bar{\lambda}, \quad (4)$$

where  $\bar{v}$  is the mean Doppler velocity and  $\bar{\lambda}$  is the average radar wavelength. Therefore, the mean Doppler velocity can be estimated from the argument of  $R_{2\delta}$  as

$$\hat{v} = -\frac{\bar{\lambda}}{8\pi\delta}\arg(R_{2\delta}). \quad (5)$$

Comparing this formula to the classical pulse-pair estimator (e.g., equation 6.19 in Doviak and Zrnić 1993), we can see that the outlined processing is equivalent to using a uniform PRT of  $2\delta$ , a quantity that can be made arbitrarily smaller without changing the “base” PRT  $T$  that determines the maximum unambiguous range.

### 3.3 Ambiguity Mitigation with ADPDF Techniques

The performance of ADPDF1, ADPDF2, and ADPDF3 in terms of range and velocity ambiguities can be characterized as follows. Assuming that  $\delta \ll T$ , the maximum unambiguous range is

$$r_a \approx cT/2 \quad (6)$$

and the “extended” maximum unambiguous velocity is

$$v_a = \bar{\lambda}/8\delta. \quad (7)$$

Hence, the range-velocity product is given by

$$r_a v_a = \frac{cT}{2} \frac{\bar{\lambda}}{8\delta} = \frac{c\bar{\lambda}}{8} \left( \frac{T}{2\delta} \right), \quad (8)$$

which compared to the classical single-frequency, uniform-PRT range-velocity product (Doviak and Zrnić 1993), reveals an improvement by a factor of  $T/2\delta$ . Note that this factor can be made arbitrarily large by adjusting the value of  $\delta$ . However, as we will see next, the ratio  $T/\delta$  also controls the errors of estimates from (5).

### 3.4. Performance of the ADPDF Doppler Velocity Estimator

A priori, it seems that ADPDF techniques could be used to arbitrarily increase the range-velocity product. However, another critical measure of performance is given by the statistical errors of the estimator (5). These are evaluated next via simulations.

Time-series data are simulated using Zrnić's method (1975). For distributed scatterers, if the frequencies from each channel are spaced by more than the inverse of the pulse width (i.e., such that the spectra do not overlap), the underlying random processes for each channel are uncorrelated (Ishimaru 1978). In this case, time-series data simulations for each channel can proceed independently. Our simulation assumes that: (1) transmission and reception paths are perfectly matched for the two frequency channels and (2) receiver filters ideally reject out-of-band signals. At first, a very short (uniform) PRT is chosen for both channels such that by “dropping” appropriate samples we can simulate the ADPDF sampling depicted in Fig. 1.

Fig. 2 shows the normalized standard deviation of ADPDF velocity estimates as a function of the normalized spectrum width for high signal-to-noise ratios (SNR) and

different values of  $T/\delta$ . Errors of velocities computed using classical, single-frequency, uniform PRT processing (UPRT) are included for comparison. From this figure, it is evident that errors of ADPDF velocity estimates increase with the  $T/\delta$  ratio. However, unlike velocity errors from UPRT, ADPDF velocity errors blow up for medium to large spectrum widths, making the estimates impractical in typical operational environments.

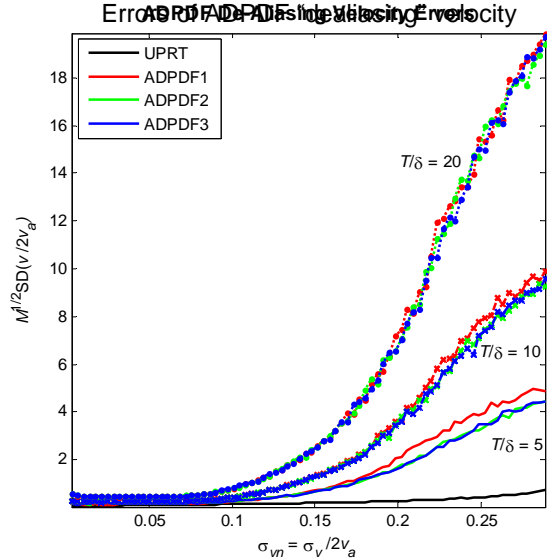


Fig 2. Normalized standard errors of ADPDF and UPRT velocity estimates vs. the normalized spectrum width.

#### 4. ADPDF Velocity Dealiasing

ADPDF velocities are unambiguous on a Nyquist interval that is  $T/2\delta$  times larger than what is achievable with a uniform PRT  $T$  and classical signal processing techniques. However, the statistical errors of such velocity estimates increase quite rapidly as the spectrum width increases. In this section we explore three solutions to this problem.

##### 4.1. ADPDF “dealiasing” velocity

Unlike velocity estimates from (5), Doppler velocity estimates from the autocorrelations at lags readily available from either frequency channel (e.g., lag  $T$  for ADPDF2) have acceptable errors, but are aliased into smaller Nyquist intervals. Therefore, the less accurate, non-aliased Doppler velocity estimate from  $R_{2\delta}$  (herein referred to as the “dealiasing” Doppler velocity estimate) can be used to determine the correct Nyquist interval for the more accurate but likely aliased Doppler velocity estimate from the autocorrelations at available lags for either channel (herein referred to as the “base” Doppler velocity estimate). As a result, the dealiased Doppler velocity estimate inherits the errors from the “base” velocity estimate and we can tolerate the higher errors of the “dealiasing” velocity. Standard errors of the “base” velocity estimates are shown in Fig. 3 for the three ADPDF techniques as a function of the normalized spectrum width for high SNR and different values of  $T/\delta$ . As before, UPRT errors are shown for comparison. Clearly, these estimates should meet operational requirements as their errors are similar or lower than those obtained with classical estimators (UPRT).

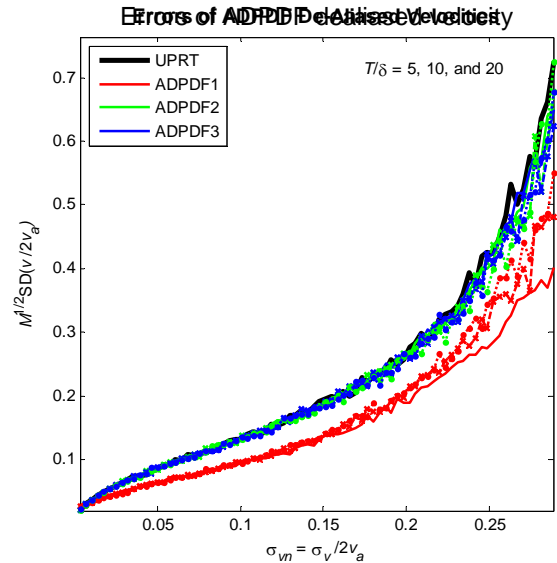


Fig 3. Normalized standard errors of dealiased ADPDF and UPRT velocity estimates vs. the normalized spectrum width.

##### 4.2. Staggered PRT velocity dealiasing

Another way to exploit the diversity of available lags for Doppler velocity estimation is by processing the signals as in the staggered PRT technique such as described by Torres et al. (2004). Instead of estimating a Doppler velocity from (5), we can use any pair of lags to obtain two velocity estimates with lower errors. The velocity difference is used as the input to a set of dealiasing rules which can be pre-computed for an arbitrary PRT ratio. These rules are used to determine the correct Nyquist co-interval for the Doppler velocity corresponding to the more accurate estimate (i.e., the estimate corresponding to the shorter PRT).

For PRT ratios of the form  $m/m+1$ , the dealiasing-rule based estimator produces the same results as the estimator based on the ratio of the two autocorrelations (e.g., Zrnić and Mahapatra 1985). For example, for ADPDF2, this estimator is given by

$$v = \frac{\lambda}{8\pi\delta} \arg [R(T_1 - 2\delta)R^*(T_1)]. \quad (9)$$

However, for other PRT ratios, this estimator does not always lead to a maximum extension of the Nyquist velocity predicted by the theory (Torres et al. 2004). As an interesting point, the reader should note the remarkable similarities between the quantities inside the  $\arg(\cdot)$  function in equations (4) and (9).

##### 4.3. Triple PRT velocity dealiasing

In the case of ADPDF2 and ADPDF3, we can obtain velocity estimates from three readily available lags (i.e.,  $T-2\delta$ ,  $T$ , and  $T+2\delta$ ). These velocity estimates can be used in a dealiasing scheme like the one introduced by Tabary et al. (2006). Velocity dealiasing is accomplished via a “clustering” algorithm. That is, from all possible aliases for the three estimated velocities we pick the “cluster” that minimizes the root-mean-square error. Again, the velocity with the lowest errors (i.e., the one corresponding to the shortest PRT) is selected as the “base” velocity to dealias.

The advantage of this scheme over staggered PRT is that by carefully selecting the PRTs, the Nyquist velocity can be extended much further.

### 5. Performance of ADPDF Techniques

Note that the dealiasing procedures described in the previous section are designed for “perfect” estimates and they have a common problem. As the errors of “dealiasing” velocities increase, these algorithms are more likely to fail by dealiasing the “base” velocity into the wrong Nyquist co-interval; we refer to this as a velocity dealiasing error. The performance of ADPDF techniques is directly related to the performance of the chosen velocity dealiasing algorithm. Therefore, the velocity dealiasing error rate (VDER) will be used to characterize the performance of ADPDF techniques in a simple and concise manner.

Simulations are repeated for a typical range of spectrum widths (0 to 8 m/s for C band and  $T = 1$  ms) and three values of  $T/\delta$  ( $T$  is 1 ms and  $\delta$  is varied to get ratios of 5, 10, and 20). The number of samples is  $M = 64$ . The SNR is set at 20 dB, and the relative frequency spacing between channels  $\Delta f/f_1$  is 0.1% (note that  $\Delta f$  this is always larger than the inverse of the pulse width for the frequency bands of interest). For every set of varying parameters, 1000 realizations of time-series data are generated and processed through each technique. Statistics are plotted as a function of the normalized spectrum width,  $\sigma_{vm} = \sigma_v/2v_a$ , where  $v_a$  is the maximum unambiguous velocity corresponding to UPRT (i.e.,  $v_a = \lambda/4T$ ). Thus, plots are equally applicable to the X, C, or S radar frequency bands. Similarly, standard deviations are normalized by the square root of the number of samples  $M^{1/2}$  and UPRT’s Nyquist co-interval,  $2v_a$ .

The VDER is determined by measuring the percentage of cases for which dealiased velocities depart from the true mean Doppler velocity by more than  $v_a$  (smaller departures are assumed to be associated with statistical errors of the “base” estimate); these are plotted as a function of the normalized spectrum width. For reference purposes, spectrum width axes corresponding to  $T = 1$  ms and X, C, and S radar frequency bands are included.

Fig. 4 shows the performance of ADPDF1, ADPDF2, and ADPDF3 using the ADPDF “dealiasing” velocity method (section 4.1). Note that the performance deteriorates with the  $T/\delta$  ratio and is equivalent for all techniques. Since the VDER increases with the normalized spectrum width, diminished performance is also observed for smaller wavelengths. For example, a given normalized spectrum width is about three times as large at X band than it is at S band so the performance of ADPDF techniques at X band deteriorates three times as quickly as it does for S band. Assuming that the maximum tolerable rate of velocity dealiasing errors is 5% (in practice, this number would depend on the effectiveness of other velocity dealiasing methods, such as techniques based on spatial continuity) and for a minimum SNR of 20 dB (which is normally the case in severe weather), the maximum spectrum widths that limit the usability of these ADPDF techniques for X, C, and S bands are given in Table 1.

Because the statistical performances of ADPDF1, ADPDF2, and ADPDF3 are essentially equivalent, we have

the freedom to choose among these variations based on other considerations. For example, ADPDF2 can be regarded as more attractive than ADPDF1 in the sense that it preserves a uniform PRT on one of the frequency channels. Therefore, it retains the ability to implement current algorithms which are typically designed to work on uniform PRTs. ADPDF3 could be deemed even more attractive since the selection of  $\delta$  can be made such that the minimum time between any two transmitted pulses is maximized. Hence, ADPDF3 is better suited for transmitters with more stringent duty-cycle constraints.

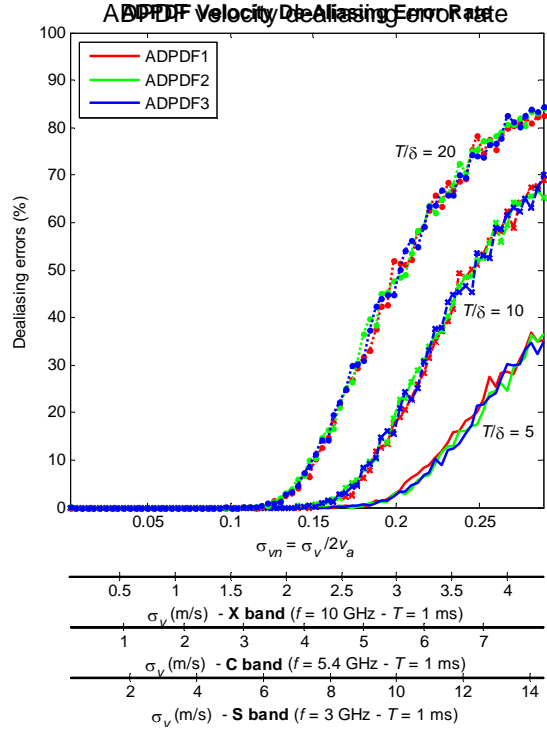


Fig. 4. ADPDF velocity dealiasing error rates as a function of the spectrum width using the ADPDF “dealiasing” velocity processing.

Band	X	C	S
$T/\delta$ 5	3.2	5.9	10.6
10	2.6	4.9	8.8
20	2.1	4.0	7.1

$\sigma_{v,max}$  (m/s)

Table 1. Approx. maximum spectrum widths that yield maximum velocity dealiasing error rates of 5% for all ADPDF techniques and typical X, C, and S radar wavelengths as a function of the  $T/\delta$  ratio for  $T = 1$  ms.

Fig. 5 compares the performance of ADPDF3 using the three velocity dealiasing methods described in section 4. Different colors are used for different  $T/\delta$  ratios and different line styles are used for the different dealiasing methods. For  $T/\delta = 5$ , the staggered-PRT processing (SPRT) provides better VDER performance and, as a bonus, an extension of the Nyquist velocity to twice the value achieved by the ADPDF “dealiasing” velocity processing (ADPDF). For  $T/\delta = 10$ , SPRT and triple PRT (TPRT) similarly provide optimum performance in terms of VDER.

Finally, for  $T/\delta = 20$ , TPRT is the best of the three.

It seems from this limited analysis that the processing of estimating the “dealiasing” velocity by combining the time series from the two frequency channels as in (5) always leads to suboptimal performance. Better performance in terms of VDER and extended Nyquist velocity is always possible with velocity dealiasing methods in which the time series from the two frequency channels are processed independently to get autocorrelation estimates. Note, however, that the performance of SPRT and TPRT may not vary “smoothly” with the  $T/\delta$  ratio as it depends on the actual ratio of the autocorrelation lags used to estimate the individual “dealiasing” velocities.

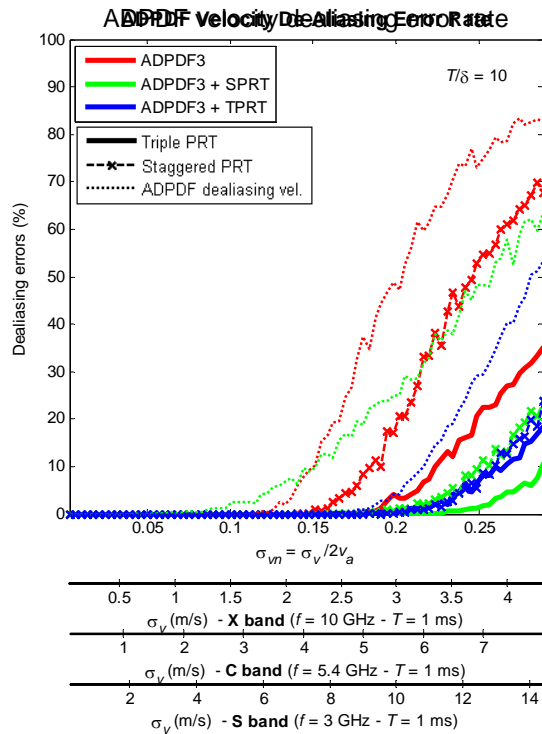


Fig. 5. ADPDF velocity dealiasing error rates as a function of the spectrum width for different  $T/\delta$  ratios using ADPDF “dealiasing” velocity, staggered PRT, and triple PRT processing.

## 7. Conclusions

This paper describes a family of range and velocity ambiguity mitigation techniques. These are termed alternating dual-pulse, dual-frequency (ADPDF) because they exploit frequency diversity in conjunction with sampling and signal processing strategies to improve the maximum unambiguous range and velocity that can be achieved through traditional signal processing methods. The main trade-off for all techniques is given by the rate of dealiasing errors vs. the extended maximum unambiguous velocity. That is, larger  $T/\delta$  ratios result in larger range-velocity products. Unfortunately, the larger the  $T/\delta$  ratio, the larger the rate of velocity dealiasing errors, and these errors limit the applicability of ADPDF techniques. The optimum  $T/\delta$  ratio and processing should be determined based on the performance of additional velocity dealiasing techniques (e.g., based on spatial continuity) that are implemented

down the signal processing chain.

ADPDF techniques are based on the same theory as more classical multiple-pulse-repetition-time techniques; however, a significant operational advantage over those is that ADPDF techniques do not necessarily exclude the implementation of other signal processing functions (e.g., those based on spectral processing) since one of the frequency channels can maintain a uniform PRT. Additionally, since samples from the two frequency channels are uncorrelated, it is possible to reduce the acquisition time by a factor of two. Another important advantage of ADPDF techniques is the possibility to share one transmitter by interlacing the transmitted pulses for the two frequency channels in a harmonious way. That is, we can maximize the time between pulses without affecting the performance of these techniques to mitigate range and velocity ambiguities. In conclusion, for weather radars that are capable of frequency diversity, ADPDF techniques could significantly improve the mitigation of range and velocity ambiguities, particularly at shorter wavelengths where this problem is exacerbated.

## References

- Doviak, R., D. Sirmans, D. Zrnić, and G. Walker, 1976: Resolution of pulse-Doppler radar range and velocity ambiguities in severe storms. Preprints, *17th Conf. on Radar Meteorology*, Seattle, WA. Amer. Meteor. Soc., 15-22.
- Doviak, R., D. Zrnić, and D. Sirmans, 1979: Doppler weather radar. *Proc. IEEE*, **67**, 1522-1553.
- Doviak, R., and D. Zrnić, 1993: *Doppler Radar and Weather Observations*. Academic Press, 576 pp.
- Glover, K. M., G. M. Armstrong, A. W. Bishop, and K. J. Banis, 1981: A dual frequency 10-cm Doppler weather radar. Preprints, *20th Conf. on Radar Meteorology*, Boston, MA. Amer. Meteor. Soc., 738-743.
- Ishimaru A., 1978: *Wave Propagation and Scattering in Random Media*. Vol. 2, Academic Press, 572 pp.
- Tabary, P., F. Guibert, L. Perier, and J. Parent-du-Chatelet, 2006: An Operational Triple-PRT Doppler Scheme for the French Radar Network. *J. Atmos. Oceanic Technol.*, **23**, 1645-1656.
- Torres, S., 2006: Range and velocity ambiguity mitigation on the WSR-88D: Performance of the staggered PRT algorithm. Preprints, *22nd International Conf. on IIPS for Meteorology, Oceanography, and Hydrology*, Atlanta, GA, Amer. Meteor. Soc., Paper 9.9.
- Torres, S., 2005: Range and velocity ambiguity mitigation on the WSR-88D: Performance of the SZ-2 phase coding algorithm. Preprints, *21st International Conf. on IIPS for Meteorology, Oceanography, and Hydrology*, San Diego, CA, Amer. Meteor. Soc., Paper 19.2.
- Torres, S., Y. Dubel, and D. S. Zrnić, 2004: Design, implementation, and demonstration of a staggered PRT algorithm for the WSR-88D. *J. Atmos. Oceanic Technol.*, **21**, 1389-1399.
- Zrnić, D., 1975: Simulation of weatherlike Doppler spectra and signals. *J. Appl. Meteor.*, **14**, 619-620.
- Zrnić, D., and P. Mahapatra, 1985: Two methods of ambiguity resolution in pulse Doppler weather radars. *IEEE Trans. Aerosp. Electron. Syst.*, **21**, 470-483.